Pediatr Radiol (2011) 41:161–175
DOI 10.1007/s00247-010-1907-0

REVIEW

Optical imaging in vivo with a focus on paediatric disease: technical progress, current preclinical and clinical applications and future perspectives

Joanna Napp · Julia E. Mathejczyk · Frauke Alves

Received: 17 May 2010 / Revised: 20 September 2010 / Accepted: 10 October 2010 / Published online: 11 January 2011

Abstract To obtain information on the occurrence and location of molecular events as well as to track target-specific probes such as antibodies or peptides, drugs or even cells non-invasively over time, optical imaging (OI) technologies are increasingly applied. Although OI strongly contributes to the advances made in preclinical research, it is so far, with the exception of optical coherence tomography (OCT), only very sparingly applied in clinical settings. Nevertheless, as OI technologies evolve and improve continuously and represent relatively inexpensive and harmful methods, their implementation as clinical tools for the assessment of children disease is increasing. This review focuses on the current preclinical and clinical applications as well as on the future potential of OI in the clinical routine. Herein, we summarize the development of different fluorescence and bioluminescence imaging techniques for microscopic and macroscopic visualization of microstructures and biological processes. In addition, we discuss advantages and limitations of optical probes with distinct mechanisms of target-detection as well as of different bioluminescent reporter systems. Particular attention has been given to the use of near-infrared (NIR) fluorescent probes enabling observation of molecular events in deeper tissue.

J. Napp · J. E. Mathejczyk · F. Alves
Department of Molecular Biology of Neuronal Signals,
Max-Planck-Institute for Experimental Medicine,
Hermann-Rein-Str. 3,
37075, Göttingen, Germany

J. Napp · F. Alves (✉)
Department of Hematology and Oncology,
University Medical Center Göttingen,
Robert-Koch-Str. 40,
37075, Göttingen, Germany
e-mail: falves@gwdg.de

Keywords Optical imaging · Fluorescence imaging · Bioluminescence imaging · Child

Introduction

In recent years, various in vivo imaging technologies have been increasingly used to monitor biological processes and to understand the complexity of diseases. Many of them progressively find application in clinical procedures allowing earlier and more precise diagnosis. Nevertheless, none of them provides comprehensive information since each imaging technique relies on different mechanisms for signal generation and thus has limitations e.g., with respect to spatial resolution, penetration depth, quantitative information and detection sensitivity, but also to safety hazards and costs. Therefore, each technique possesses a unique combination of advantages and disadvantages that affects its selection for use in a particular study. Imaging techniques such as ultrasound (US), computed tomography (CT), and magnetic resonance imaging (MRI) are used to visualize morphological properties of tissue, whereas techniques such as positron emission tomography (PET), single-photon emission computed tomography (SPECT) and optical imaging (OI) with fluorescence or bioluminescence as sources of contrast allow information to be obtained on the location of molecular events or to follow-up distribution of applied probes in living organisms [1]. To take advantage of the strengths of different imaging devices, multimodal-imaging strategies demonstrate attractive tools for preclinical and human applications. In this review, key characteristics and technical progress of OI as well as the current use and potential impact of OI methods in preclinical research and in clinical management of children are discussed.

Fluorescence imaging

Fluorescence imaging is based on the detection of photons, emitted by a substance that has absorbed light or other electromagnetic radiation of a different wavelength. Fluorescence occurs when an orbital electron of a molecule, atom or nanostructure relaxes to its ground state by emitting a photon of light after being excited to a higher quantum state. Usually, emitted light has a longer wavelength, and therefore a lower energy, than the absorbed radiation.

The majority of OI systems are based on planar measurements of fluorescence typically overlaid with photographic images of the surface of the scanned object. Those devices usually consist of an excitation source such as a multispectral light source or a laser of appropriate filters and a camera. As the excitation source and the detector can be placed either on the same side or on opposite sides of the scanned object, planar imaging can be performed in an epi-illumination modus, known as fluorescence reflectance imaging (FRI), in which the returning fluorescence response is measured and, less expanded, transillumination imaging in which the light shining through the object is collected [2]. Although not as widely used, transillumination attains important benefits over epifluorescence imaging such as improved depth sensitivity and contrast, as it carries information from the entire volume of the sample in comparison to reflectance measurements that are surface-weighted [3].

An innovation in fluorescence imaging was the implementation of time-domain imaging that allows calculation of fluorescence lifetime, a parameter that characterizes a fluorescent probe by describing the average amount of time a fluorophore spends in its excited state before returning to the ground state. In this technique a pulsed laser diode is used as an excitation source. The first photon response is measured time-resolved with a photomultiplier tube after each single excitation pulse and used to calculate the fluorescence lifetime. As lifetime is a specific characteristic of particular fluorescent probes, the determination of lifetime values permits the identification of specific, probe-derived signals and their separation from unspecific background fluorescence (Fig. 1) or the discrimination of various fluorophores with distinct fluorescence decay rates [4, 5].

In vivo fluorescence intensity measurements strongly depend not only on the probe's spectroscopic properties and/or its concentration within the tissue but also on parameters, such as depth of the fluorescence source within the tissue or on the density and homogeneity of the tissue itself. Therefore, traditional planar imaging of the fluorescence response projected on the surface of living objects can offer only semi-quantitative data. In contrast, recent developments in tomographic fluorescence imaging including fluorescence-mediated tomography (FMT), optical projection tomography (OPT) and diffuse optical tomography (DOT) provide 3-D information about the fluorescence distribution, based on accurate theoretical models of photon propagation including absorption and scattering of both excitation and emission light in tissues. The resulting tomographic fluorescence maps reconstructed after mathematical processing allow relatively accurate and true quantification of the data independent of the depth of the fluorescence source and have been successfully applied in preclinical models e.g., to monitor cancerous tissue [6, 7], to calculate vascular volume fractions [8] and to visualize and quantify pulmonary inflammation in vivo [9]. Although novel approaches for improved quality of 3-D fluorescence imaging, such as DOT-guided FMT [10] are continuously evolving, the impact of heterogeneity of living objects and tissue optical properties on the mathematical models of image reconstruction still requires further modification.

In order to image down to subcellular resolution, different microscopic techniques have adapted to in vivo fluorescence

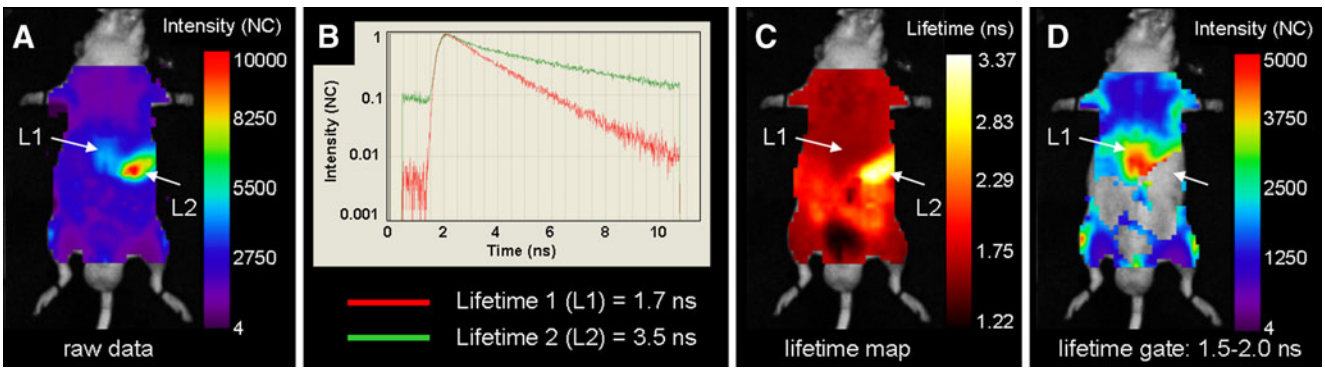

Fig. 1 Fluorescence lifetime imaging in vivo. **a** NIRF raw scan data of a living mouse with a pancreatic tumour obtained 24 h after application of an anti-matriptase antibody shows signals with a probe-specific lifetime of 1.7 ns detectable over the tumour area (*L1*), as well as nonspecific signals (3.5 ns) over the stomach area (*L2*). **b** A representative photon time-of-flight histogram; each line corresponds to a single point on the raw scan. **c** Lifetime map displays the distribution of the different fluorescence species. **d** After gating the lifetime to 1.5–2.0 ns only specific, probe-derived fluorescence over the tumour is detectable

imaging enclosing two- and multiphoton microscopy or confocal microscopy. In addition, optoacoustic (photoacoustic) techniques evolved for the microscopic imaging of intact tissue. In comparison to whole-body imaging systems, microscopic devices operate with small fields of view and therefore allow imaging only in selected parts of tissues. Furthermore, because of the very limited penetration depth, the microscopic imaging of deeper tissues requires invasive procedures, e.g., the use of implantable windows, endoscopes or miniaturized fibre-based catheters. Such micro(endo)scopic techniques allow functional information on dynamic processes within tissues and organ systems to be obtained that are maintained in their natural state and provide "optical biopsies" of living tissues by avoiding the risks, costs and time delay involved in tissue resection.

Confocal (intravital) microscopy is relatively inexpensive and user-friendly. This method relies on a laser source that focuses on a single spot in the sample and the light emitted from this focal point is imaged through a pinhole onto a detector. Here, phototoxicity can be a limiting factor especially during long scanning times. As the optical penetration of confocal microscopy into tissues is limited to 200–500 μm, its clinical application is restricted to examinations of superficial structures such as visualization of melanocytic skin tumours [11]. Two- or multiphoton microscopy imaging is based on the simultaneous absorption of two or more photons under high light irridance. Due to its capacity for deep penetration of up to 800 μm, its efficient light detection and the potential to image tissue for hours in high spatial resolution, this technique is increasingly used as an efficient and less phototoxic imaging approach to investigate biological processes in deep and vital tissues within their intact environment [12].

Optical coherence tomography (OCT), that uses broadband NIR light sources with considerable penetration of about 2–3 mm into tissue, is one of the most promising techniques for biomedical tissue imaging. In clinical practice OCT is applied mainly to provide information on easily accessible tissues such as skin, gastrointestinal and retinal pathology in situ and in real time. It provides optical biopsies with resolutions approaching those of excisional biopsy and histopathology based on the detection of inhomogeneities [13]. Tissue microstructure is revealed by differentiating between scattered and transmitted, or reflected photons [14]. As it enables measurement of tissue pathology with resolution of several micrometers (1–15 μm) OCT perfectly fills the gap between microscopic and whole-body imaging techniques.

Based on the measurement of optical absorption in tissues photoacoustic microscopy that detects absorbed photons ultrasonically through the photoacoustic effect is also an emerging tool for in vivo imaging [15]. This method provides multiwavelength imaging of optical absorption and permits better spatial resolution than pure optical imaging since the imaging depth is beyond ~1 mm [16].

Endogenous fluorescent labels/genetic reporters

The revolution in the development of fluorescence imaging was the identification of the first fluorescent protein, green fluorescent protein (GFP) from jellyfish, purified and characterized in the early 1970s [17]. However, it took almost 20 years until the whole GFP was cloned and sequenced [18]. Today fluorescent proteins exist in many colours that span the visible spectrum from deep blue to deep red. The utility of these genetically encoded probes for in vivo fluorescence labelling has been demonstrated in a variety of different cellular systems and transgenic organisms. For example, interactions between host and tumour environment have been studied in GFP-expressing transgenic mice transplanted with red fluorescent protein (RFP)-expressing cancer cells. This approach allowed the distinction between cancer and host cells including host blood vessels, lymphocytes, tumour-associated fibroblasts, macrophages, etc. and was shown to be a powerful tool to study the efficacy of drugs on each type of cell [19].

When selecting among the many colour variants available for in vivo imaging, it is important to consider fluorescent proteins that are very bright, most photostable and those requiring minimal exposure to excitation to maintain cell viability [20–22]. Fluorophores absorbing and emitting in the NIR wavelength region between 650 nm and 900 nm are particularly valuable for in vivo imaging, since this light spectrum not only benefits from less autofluorescence but is also only poorly absorbed by haemoglobin, water and lipids, allowing up to 2-cm tissue penetration [23]. Accordingly, endogenous gene reporters for whole-body near-infrared fluorescence (NIRF) imaging in preclinical studies have been expressed in mammalian cells such as infrared-fluorescent proteins (IFPs), engineered from a bacterial phytochrome [24] or the bright far-red fluorescent protein Katushka and mKate, the monomeric form of Kathushka [25]. Nevertheless, the clinical use of endogenous fluorescent labels has its limitations due to the need for cell-engineering and to the lack of any information on its long-term side effects.

Exogenous fluorescent probes

The majority of the in vivo NIRF imaging studies involve application of fluorescent probes that usually target specific markers or molecular events in model organisms. Prereq-

uisites here are efficient fluorescent labels, which define the detection limit and dynamic range of the method. Such fluorophores should have NIR absorption- and emission-maxima, a high molar absorption coefficient at the excitation wavelength, high fluorescence quantum yield and sufficient thermal and photochemical stability [21, 22]. Moreover, suitable fluorescent dyes have to be soluble and stable in buffers and body fluids and the resulting probe should reveal maximal targeting efficiency by reduced nonspecific binding and low toxicity [22]. The ability to employ simultaneously different fluorescent probes in combination with multiple imaging channels and thereby facilitating the visualization of more than one target and various biological processes in one animal is one functional benefit of fluorescence over the majority of other in vivo imaging modalities [26].

There are relatively few classes of NIRF dyes available for in vivo imaging including organic dyes such as phthalocyanines, cyanine dyes and squaraine dyes. Most of the currently used NIR fluorochromes are cyanine dyes containing two heterocyclic rings linked by a polymethine bridge e.g., Cy-, DY-, IR-dyes, or AlexaFluor-dyes, cypate and indocyanine green (ICG) [27]. Despite ongoing efforts in the design of novel fluorescent probes up to now only one fluorescent dye, ICG, has been approved by the Food and Drug Administration-USA (FDA) for use in patients e.g., for the intraoperative assessment of reconstructed vessels in living-donor liver transplantations [28] or in ophthalmic angiography [29].

Although organic fluorophores represent the major group of the fluorescent probes for in vivo application, they usually suffer from low fluorescence quantum yields and limited sensitivity and photostability as well as from agglomeration and susceptibility to environmental changes in blood or tissues. Moreover, many of them possess a certain level of toxicity that hampers their in vivo application. One of the solutions is enclosure of fluorescent dyes in nanomaterials, such as polymeric nanoparticles (NPs), which can be fabricated from a multitude of materials in a variety of compositions and doped with different fluorophores. This has the advantage of protecting the potentially toxic fluorophores from the environment and offers improved fluorophore stability due to reduced interactions with the environment, e.g., solvent molecules, chemically reactive species or quenching agents [30]. The main advantage of using NPs is their large surface areas allowing easy modification with a wide range of imaging moieties including several surface modifications for multi-modal detection and/or drug delivery [31], but also surface attachment of target-specific bioligands or polymeric compounds such as polyethylene glycol (PEG). In particular, PEGylation is of particular interest as it strongly influences the pharmacokinetics of NPs by reducing clearance by the reticuloendothelial system and increasing plasma half-lives of the NPs but also their stability and water solubility while reducing their immunogenicity [32, 33].

Nevertheless, many presently available NP-formulations comprise potentially toxic elements. In spite of growing efforts to reduce side effects, such as using biodegradable coatings, the biodistribution, behaviour and risks of using NPs in living organism still have to be studied [34].

Luminescent semiconducting nanocrystals, quantum dots (QDs), which can readily be conjugated to targeting molecules (e.g., antibodies), are also increasingly used as fluorescent labels for in vivo imaging. Unlike organic dyes, QDs can be excited over a broad wavelength and their optical properties are controlled by the constituent material, particle size and dispersity, shape and surface chemistry. The use of QDs for in vivo imaging is also hampered by the contradictory reports on their toxicity [22].

Three major classes of fluorescent reporters can be distinguished, based on their mechanisms of target-detection: (1) nontargeted contrast agents that nonspecifically accumulate in certain tissues, (2) target-specific fluorescent labels that are directed against molecular and/or disease-specific markers and (3) responsive/activatable "smart" probes for the detection of molecular events such as enzymatic activity or pH sensing.

Nontargeted fluorescent probes

Nontargeted (passive) contrast agents deliver fluorescent probes to a certain tissue without specifically binding to cellular targets. There are two major targets for passive imaging: blood vessels and tumour tissue. Accumulation of non-targeted probes at the tumour sites is achieved by pathologically enhanced endocytic activity, hyperpermeable and leaky vasculature and lack, or abnormal lymphatic drainage, attributes, which can be summarized as the enhanced permeability and retention (EPR) effect. As the abolished integrity of the endothelial barrier in the vasculature is an integral part of different diseases, nontargeted contrast agents have been used to visualize cancer but also other pathological sites such as inflammation, rheumatoid arthritis or infarction. Since a sufficient blood circulation time is essential for the successful delivery of probes, the longevity of contrast agents in the blood stream is necessary to permit accumulation within the targeted tissue.

Several nonspecific contrast agents are commercially available, such as ICG systematically used for ophthalmic angiography in clinical settings [35, 36] and to imagine blood flow using video angiography during cerebral surgery in clinical trials [37]. An NIRF blood-pool contrast agent AngioSense, consisting of PEGylated graft copolymers and indocyanine-type fluorophore, can be used for monitoring

of blood vessels (Fig. 2) and phenomena such as blood leakage in tumours, as well as for visualization of oedema and inflammation [8]. Also fluorophore-doped NPs, such as viral NPs [38], liposomes [39] and QDs [40] have been used as tools for passive vascular imaging in preclinical settings. Here, size, composition and surface hydrophilicity of NPs, can influence their blood circulation time.

Targeting probes

The majority of imaging probes consist of fluorophores or fluorescent nanomaterials attached to ligands, e.g., antibodies, antibody fragments or peptides targeting a tissue- or disease-specific molecule/-s. In recent years reams of monoclonal antibodies conjugated to fluorescent labels have been used for in vivo imaging. One example is trastuzumab (Herceptin), a well-characterized and clinically applied humanized anti-HER2/neu monoclonal antibody, fused to Cy5 (Fig. 3) [41] Cy5.5 [42] or ICG [43] for detection of HER2/neu-overexpressing tumours in mice. Our own work demonstrated the use of different Cy5.5 labelled monoclonal antibodies in orthotopic mouse tumour models, for example, to assess the expression of the tumour-associated protease, matriptase in pancreatic tumours [4] (Fig. 1) or to preclinically evaluate antibodies [44, 45] for their use in anti-tumour therapies.

Emerging progression in recombinant DNA technologies raced the optimization of the traditional monoclonal antibodies used for imaging and treatment by new structural designs including production of chimeric and humanized antibodies or recombinant antibody fragments [46]. However, several aspects have to be considered when applying antibodies, antibody fragments or peptides for in vivo imaging. First of all, the biodistribution and pharmacokinetics of ligands is strongly influenced by their size. Comparably large whole antibodies are slowly cleared from the blood circulation and only slowly penetrate into tissues, which can result in a high background and poor tissue-to-background contrast [47]. Molecules smaller than antibodies such as antibody fragments or peptides, can be advantageous for in vivo targeting because of their rapid blood clearance resulting in better signal-to-background ratios. If clearance is too fast, however, small ligands will not have sufficient time to penetrate target tissues before they are removed from the blood pool. In addition, in contrast to whole monoclonal antibodies, which usually arise from mice, engineered antibody fragments are expected to be only minimally immunogenic in human applications. Also, the affinity of a particular ligand for its antigen can influence its diffusion into the target tissue. High affinity increases the amount of ligand in the targeted tissue only up to a certain threshold, above which tumour penetration is reduced or even inhibited [48]. This occurs due to the (too) strong interaction and usually irreversible association of the ligand with its antigen molecules present in close proximity to the blood vessels, thereby avoiding further diffusion of the ligand into the tissue. This so-called binding site barrier effect was postulated by Weinstein in early 1990s and is especially true for large and poorly vascularized tumours [48, 49]. Furthermore, other factors such as systemic clearance of probes, density of cells in the desired tissue, or high interstitial pressure e.g., within tumours have to be considered when using antibodies, antibody fragments or peptides for tissue-targeting [50]. Intermediate-size molecules with reduced blood circulation times, however long enough to

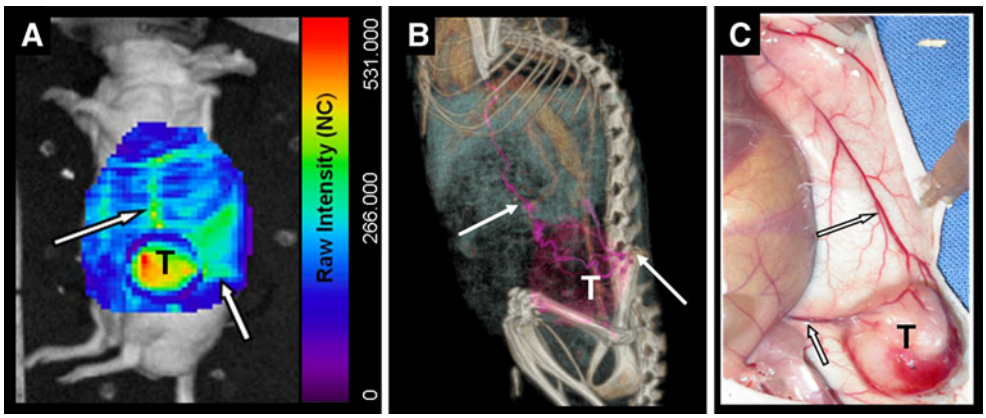

Fig. 2 Visualization of tumour vascularization using a nontargeted blood pool contrast agent. **a** NIRF image acquired 1 h after intravenous injection of AngioSense^{680} into a mouse bearing a glioblastoma xenograft. Strong fluorescence is measured over the tumour (*T*) indicating high vascularization. Two large tumour-supplying vessels show strong fluorescence (*arrows*). **b** High-resolution anatomical scan, performed by flat panel volume CT (fpVCT), 90 s after intravenous application of 150 µl iodine-containing blood pool agent confirmed the localization of the same two large blood vessels (*arrows*) detected in (**a**), and also shows smaller tumour vessels (*pink*). **c** Macroscopic image of the same mouse confirms the presence of the two large vessels (*arrows*)

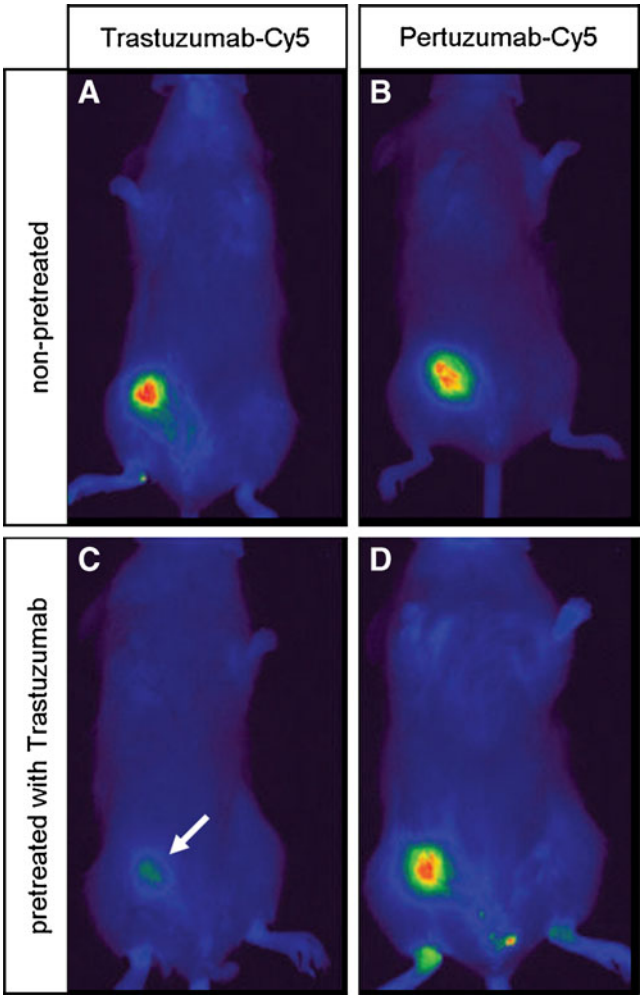

Fig. 3 Evaluation of trastuzumab and pertuzumab tumour binding by NIRF imaging. Specific binding of (**a**) trastuzumab-Cy5 and (**b**) pertuzumab-Cy5 antibody-conjugates to HER2/neu-expressing mammary tumours in vivo. Both mice show comparable NIRF signals at the tumour site. **c** and **d** When mice were pretreated with unlabelled trastuzumab, no tumour staining was seen with trastuzumab-Cy5 (**c**, *arrow*), whereas pertuzumab-Cy5 treatment showed nonaffected staining intensity indicating different binding sites for the antibodies on the tumour site (**d**). The illustration is reprinted with kind permission from Cancer Research and with courtesy of Discovery Oncology, pRED, Roche Pharma, Penzberg from reference [41] (Figure 3)

allow tissue-specific accumulation seem to be the optimal probes. For example, anti-HER2/neu affibody molecules (small high affinity proteins of few kDa) labelled with AlexaFluor dyes allowed visualizing HER2-expressing tumours without interfering with the therapeutic efficacy of Herceptin [51]. Further, NIRF-labelled ligands such as vascular endothelial growth factor (VEGF) [52] or folic acid, an agonist binding to the folate receptor [53], have been used to monitor tumour angiogenesis and arthritis in vivo, respectively. A peptide-dye conjugate consisting of cyclic arginine-glycine-aspartic acid pentapeptide attached to Cy5.5 (RGD-Cy5.5) was applied to determine integrin expression in vivo with high specificity and long-lasting tumour accumulation [54]. Furthermore, fluorophore-labelled toxins, such as Cy5.5-labelled chlorotoxin, a small peptide from the venom of the deathstalker scorpion *Leiurus quinquestriatus*, have been applied as optical probes for NIRF imaging. Cy5.5-labeled chlorotoxin enabled delineation of malignant glioma, medulloblastoma, prostate cancer, intestinal cancer and sarcoma from adjacent non-neoplastic tissue in mouse models and to detect metastatic cancer foci as small as a few hundred cells in lymph channels [55].

Activatable probes

A group of "smart" activatable or responsive probes evolved to detect and quantify target-specific enzymes, molecular processes as well as changes in oxygen or pH levels in living organisms over time. Such probes usually display "switch-on" or increase in the fluorescence emission or shifts in the absorption and/or emission spectra upon specific processes, such as cleavage of the probe or changes in the probe-environment.

Protease-sensing

First concepts of protease-sensing probes, polymer-based optically quenched activatable probes for tumour imaging were introduced by Weissleder's group [56]. They consist of fluorochromes quenched by their high density, grafted to an enzymatically cleavable polymer backbone that functions in vivo as a long-circulating delivery carrier. NIRF signals are generated as a result of lysosomal cysteine/serine protease activity in cells after probe internalization [56]. Sequentially, activatable probes specific for certain proteases such as cathepsin-D [57] and -K [58], caspase 1 [59], matrix metalloproteinases (MMPs) [60] or urokinase-type plasminogen activator (uPA) [61], have been developed. They are all based on protease-specific peptide substrates introduced between the polymer backbone and quenched fluorophore molecules. Further constructs are caspase-sensing NIRF NPs for apoptosis imaging. They consist of a cleavage peptide (DEVD) and Cy5.5 both attached to a deoxycholic acid (DOCA) polymer backbone that is cleaved by caspase-3 and -7 [62].

PEG or other polymers usually conjugated to activatable probes efficiently increase the probe stability and blood circulation time, although with some disadvantages. The large molecular size of the polymer substrates (>100,000 molecular weight) may reduce permeation into cells and many PEG molecules might interfere with the interaction between the peptide substrate and the target enzyme [63, 64].

A nonpolymeric small peptide selfquenched probe was applied for the assessment of activity of matriptase, a serine

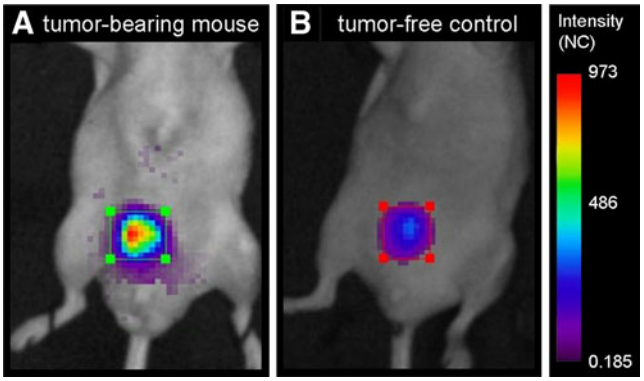

Fig. 4 Measurement of matriptase activity using a nonpolymeric activatable probe. Fluorescence intensity was measured over the bladder area of a mouse (**a**) bearing an orthotopic pancreatic tumour and of a tumour-free control (**b**) approximately 60 min after intravenous injection of a selfquenched matriptase-activatable probe. Enzymatic activity of matriptase in tumour-bearing mice was assessed by increase in the fluorescence intensity in comparison to the control

protease expressed on the surface of tumour cells (Fig. 4). Due to the small molecular weight of the probe consisting of two DY-681 molecules attached to a short peptide containing a matriptase cleavage site, no measurable accumulation of the substrate in tumour tissue was achieved. Therefore, the activity of matriptase and its inhibition was assessed by determination of fluorescence intensity of the cleaved substrate accumulating in the bladder (Fig. 4) [4]. Dye molecules can also be attached to metal NPs such as gold (AuNPs) in order to produce protease activatable probes such as a MMP-cleavable AuNPs probe for tumour imaging. Due to electronic interactions between the chromophore and AuNPs, this binding results in very strong quenching of the fluorescence [63].

Quenched probes for signal amplification

Another group of "smart" probes utilizes the dye quenching-dequenching principle for signal amplification. Similar to protease-sensors, these probes contain also a high density of dye molecules that are attached to a ligand; here the dequenching occurs after cell internalization of the ligand-dye complex. One example is a nonpolymeric agent consisting of two independent domains, an integrin recognizing RGD motif as cell targeting domain and the imaging domain composed of a Cy5 dye, a cleavable bond and a quencher. Probe activation only occurs after RGD-integrin mediated probe internalization followed by intracellular release of the fluorophore into the lysosome [63]. A similar approach was described by Ogawa et al. [43, 65], who characterized a selfquenching probe consisting of a high number of fluorophore molecules attached to a single antibody molecule, Herceptin, that are dequenched after HER2/neu receptor mediated internalization. This kind of smart probe may have great potential for improving image contrast.

ß-galactosidase sensing

Bacterial ß-d-galactosidase (ß-gal) is the most widely used reporter gene for enzyme immunoassays in molecular biology. A variety of chromogenic and low-emitting fluorogenic substrates have been described, but first the development of NIRF probes, such as DDAOG or Gal-2SBPO (Fig. 5), facilitated ß-gal activity measurements in vivo. DDAOG is a

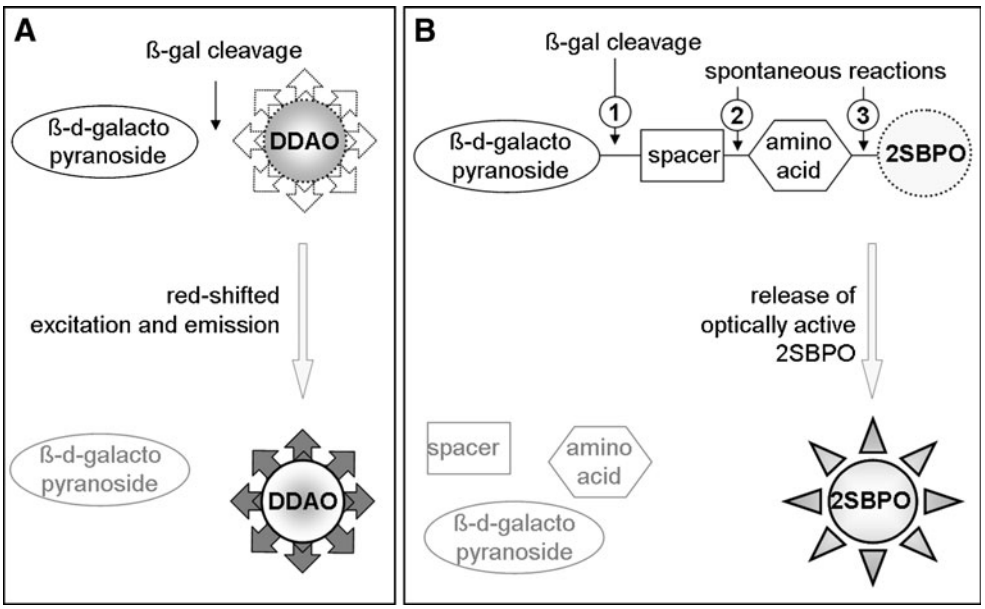

Fig. 5 ß-galactosidase sensing in vivo. **a** ß-gal triggered cleavage of DDAOG results in far red shifts of the excitation/emission peaks from 465/608 nm to 646/659 nm. **b** The optically active 2SBPO is released after a series of spontaneous reactions following the enzymatic cleavage of the ß-d-galactopyranoside from the gal-2SBPO by ß-gal. The illustration (**b**) is used with permission of ChemBioChem and was taken and adapted from Scheme 1 from reference [69]

ß-d-galactopyranoside conjugate of the DDAO (9H-(1,3-dichloro-9,9-dimethylacridin-2-one-7-yl)); the cleavage product shows a far red shifted absorption and emission spectrum, enabling its specific detection in a background of the intact probe. Although DDAOG has been successfully applied for imaging of ß-gal-expressing tumours and monitoring transgenic expression of the LacZ gene in mice, as the narrow emission spectrum of DDAO seriously overlaps with the absorption spectrum, this probe still needs improvements for efficient in vivo application [66–68]. Gal-2SBPO, a ß-d-galactopyranoside conjugate of 2SBPO (9-di-3-sulfonyl-propylaminobenzo[a]scphenoxazonium perchloride) is a dual fluorogenic and chromogenic substrate for ß-gal [69]. Enzymatic cleavage of the probe triggers a series of spontaneous reactions that result in release of optically active 2SBPO. Since the substrate emits in the far-red wavelength region, it shows promise as a reporter molecule for in vivo imaging of ß-gal activity.

pH sensing

Changes in pH are hallmarks of numerous diseases such as inflammation or cancer. For example, acidosis of the tumour microenvironment that is induced by upregulated glycolysis under hypoxic conditions is pervasive in almost all solid tumours [70]. Based on these conditions, interest for the use of pH-activatable probes in vivo arose. Currently, there are only a few NIR-emitting pH-sensitive probes available; most of the pH probes contain fluorophores that absorb and emit in the visible region. The NIR pH sensors can be divided into two groups. The first group is represented by self-quenching fluorescent pH probes in which the sensors are designed similarly to protease-sensitive selfquenchers, but contain an acid-sensitive instead of a protease-sensitive linker [71]. The second group comprises mainly cyanine- or norcyanine-based dyes, with a protonatable amine group within the chromophore, such as square-650-pH [72], or ICG- and cypate-based sensors, H-ICG and H-cypate [73]. Whereas pH sensing on tumour cells in vitro is well-established [74], measuring pH changes in vivo still remains a challenge. Here, the advantage of the activation of pH-sensitive dyes in the acidic environment is mainly used to increase the signal to background contrast either after accumulation of the probe e.g. in the tumour tissue or after receptor-mediated internalization of the dye-ligand complexes into acidic endosomal/lysosomal compartments of the target cell. In this way, by applying pH-activatable BODIPY-based conjugates Urano et al. [75] were able to reach 22-fold higher tumour-to-background ratios than using an always-on fluorescent probe. However, as the BODIPY dyes absorb in the range around 490 nm, the limited tissue penetration restricted generation of in vivo data and allowed only ex vivo measurements. Recently an in vivo enhancement of tumour contrast was achieved by application of a novel pH-activatable NIRF nanoprobe InNP1 [76]. Nevertheless, there is still demand for the development of sensitive pH indicators for measuring pH changes or to further improve tumour contrast in vivo.

Bioluminescence imaging

BLI enables a relatively robust, simple, inexpensive and extremely sensitive detection of essential biological processes in vivo in a variety of disease models. In contrast to fluorescence imaging this method is based on the detection of light produced and emitted by a living organism and it does not necessitate any external light source for excitation. However, BLI requires genetic labelling of cells with light producing enzymes (the luciferases) and as mammalian cells do not produce the luciferase-substrate responsible for the light emission, the substrate must be delivered systematically.

The most commonly used bioluminescent reporter for small animal imaging is luciferase from the firefly (*Photinus pyralis*). In an oxygen-, magnesium-, and ATP-dependent process the firefly luciferase oxidates its substrate, luciferin, whereby light is produced with a broad emission spectrum and peak intensity at ~560 nm [77]. Click beetle (*Pyrophorus plagiophthalamus*) luciferase catalyzes green to orange (546–593 nm) bioluminescence after oxidating luciferin [78]. *Renilla* (sea pansy) and *Gaussia* (marine copepod) luciferases react with the substrate coelenterazine to produce blue light (~480 nm) in an ATP-independent process [79, 80]. Moreover, lux operons from bacteria, e.g., *Photorhabdus luminescence*, emit blue light that has widely been used for BLI of bacterial infections [81]. The lux operon encodes all proteins required for bioluminescence: luciferase, its substrate and substrate-regenerating enzymes, enabling continuous light production by the system without need for exogenous substrate. Nevertheless, this autonomous light-generating system has not been successfully transferred to mammalian cells. Firefly luciferase is the preferred enzyme for BLI in vivo, since it produces more light than click beetle luciferase, has longer emission wavelength than *Renilla* and *Gaussia* luciferases and luciferin show lower background signals but a better biodistribution than coelenterazine. However, the availability of multiple luciferases is advantageous as it allows different biological processes to be monitored in parallel in vivo, using appropriate filter combinations and substrates [82].

Due to the abandonment of external illumination sources, BLI provides very high detection sensitivity and low background signals, especially when compared to fluorescence imaging where the external illumination of tissue causes endogenous particles of the animal to emit light. Already as few as ~500 cells can be reliably detected in vivo at specific anatomical sites [83]. In vivo biodistribution and pharmacology of luciferase substrates are critical parameters in regard

to detection sensitivity and reproducible quantification of BLI. Bioluminescent signals vary with time after injection of the substrate, e.g., luciferin distributes throughout an animal rapidly after injection and light produced by firefly luciferase peaks ~10–12 min after injection of luciferin and slowly decreases afterwards. To achieve comparable results, the time between injection of substrate and start of measurement as well as the dose of administered substrate should be standardized for each study [82].

Further parameters that affect the sensitivity of BLI are the wavelength of the emitted light, the expression level of enzymes in the target cell, the position of bioluminescent cells in the mouse as well as the efficiency and sensitivity of the CCD camera. A problem of planar BLI is the 10-fold loss of photon density for each centimetre of tissue depth. This creates surface-weighted images and lets the light sources closer to the surface appear brighter compared with deeper sources.

BLI can be used to study preclinically protein expression during disease progression and in response to therapy. For this purpose often transgenic animals are generated expressing luciferase either ubiquitously or under the control of a regulated promoter. As bioluminescence will occur only when the controlling promoter is active, this technique enables the monitoring of spatiotemporal changes of protein expression in vivo e.g., as applied for analysis of the heme oxygenase-1 that plays a key role in development and where disregulation is often associated with jaundice in neonates [84, 85]. Transgenic mice expressing luciferase under the control of a lobe-specific promoter were used to investigate the early onset of retinoblastoma [86] or to generate luciferase expressing haematopoietic stem cells used for the visualization of leukemogenesis after transplantation in bone-marrow-depleted mice [87]. Moreover, mice expressing luciferase fused to a region of hypoxia-inducible factor (HIF) has been used for monitoring hypoxic tissues (Fig. 6a). As hypoxia is a hallmark of many paediatric diseases, such mice can be applied in preclinical paediatric research for evaluating therapeutic agents that stabilize HIF by monitoring hypoxia [88]. A further possibility to introduce a gene encoding luciferase into a living organism is transduction with viral particles enclosing luciferase reporters that infect certain cell types to be studied. In this context a luciferase-containing avian retrovirus has been used in a transgenic mouse model expressing the corresponding retrovirus receptor to study location of haematopoietic stem cells in mice [89]. Luciferase-expressing viral vectors have further been

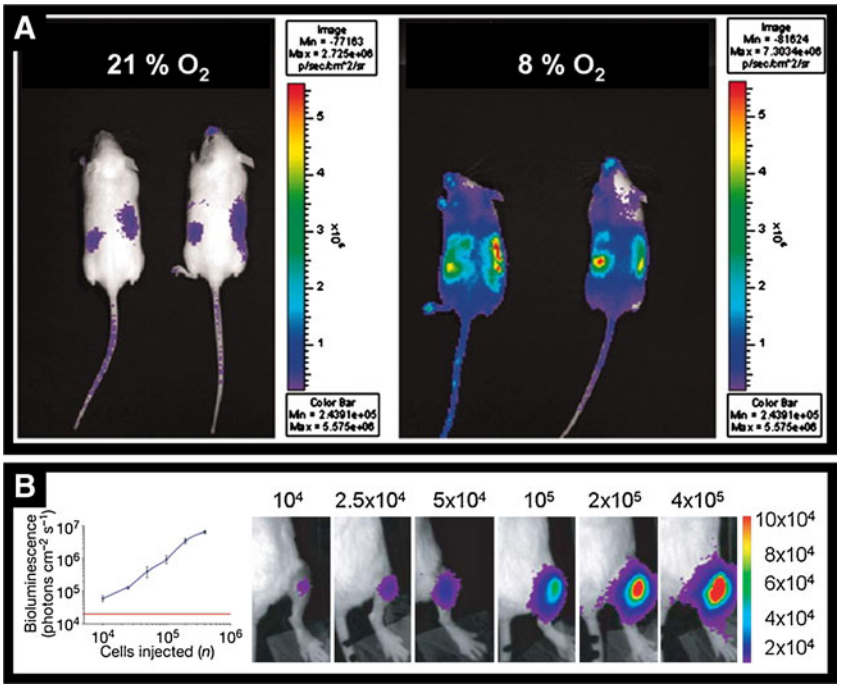

Fig. 6 BLI in animal models. **a** BLI of hypoxia. Transgenic *ROSA26* ODD-Luc/+ mice ubiquitously expressing a bioluminescent reporter consisting of firefly luciferase fused to a region of HIF that is sufficient for oxygen-dependent degradation were breathing 21% or 8% oxygen. An approximately 5- to 10-fold increase in light emission could be observed under hypoxic conditions. The illustration is reprinted with kind permission of PNAS, copyright (2006) National Academy of Sciences, U.S.A, from reference [88]. **b** Muscle stem cell engraftment monitored in vivo by BLI. Increasing numbers of luciferase-expressing myoblasts were injected into the tibialis anterior muscles of NOD/SCID recipients and imaged with BLI 2 h after injection. Here, the minimum number of cells detectable above control uninjected legs was 10,000. The bioluminescence intensity increased linearly with the number of injected cells. The illustration is reprinted with kind permission from Macmillan Publishers Ltd: [Nature], from reference [91], copyright (2008)

applied for evaluation of gene therapy for pulmonary diseases such as cystic fibrosis [90].

Moreover, transplantation of different cell types that are modified to express luciferase is widely used to monitor different processes such as tracking of muscle stem cells during muscle repair (Fig. 6b) [91]. Transplantation of cancerous cells is also commonly used to investigate tumour development, growth and therapy in a variety of animal tumour models for common childhood cancers such as lymphoma [92]. In order to identify proteins involved in leukaemia progression, BLI was applied in combination with knock-down of protein expression by RNA interference [93]. Furthermore, a bioluminescent rodent model for studying growth and therapy of brainstem tumours (one of the most severe neoplasms for children) has recently been established [94]. Luciferase-expressing mouse models of osteosarcoma, the most common primary bone tumour in children and young adults, enabled earlier tumour detection in comparison with tumour volume measurements as well as detection of lung metastases and monitoring of response to therapy in preclinical studies [95, 96].

As generation of bioluminescence in mammalian cells requires the introduction of a DNA-encoding luciferase into the target cell, which is a highly manipulative genetic intervention, it is from both a medical and ethical point of view very unlikely that BLI will ever be applied in humans. Nevertheless, because of its high specificity and sensitivity, BLI provides an effective and valuable preclinical tool to investigate distinct biological processes, to explore and better understand the biology of human diseases including distinct processes of newborn and childhood disease or to accelerate the development of possible therapeutic interventions.

Multimodal imaging

Since OI lacks any anatomical information, coregistration of data from OI imaging to anatomical structures visualized with imaging devices, such as CT, MRI, and US, is advantageous to provide complementary information in disease models. Combined MR and NIRF imaging include the use of probes consisting of NIR fluorophores conjugated to iron oxide nanomaterials or a combination of superparamagnetic iron oxide or gadolinium MR contrast agents with organic fluorophores or QDs [97, 98]. Data from FMT have been integrated to radionucleotide measurements obtained by PET [99]. Coregistration of NIRF signals and CT datasets has been reported based on the position of fiducial markers detectable by both imaging devices and software for fusion of 2-D data from FRI with 3-D data obtained from high-resolution flat-panel volume CT (fpVCT) (Fig. 7) [44]. Similar approaches have been reported for the fusion of FMT data with CT used to localize high protease activity to the vasculature in an atherosclerosis mouse model [100] and with MRI to characterize processes of pulmonary inflammation [101]. Furthermore, an approach has been developed to integrate photoacoustic microscopy and spectral-domain OCT by simultaneous volumetric microscopic imaging of both optical absorption and scattering contrasts in biological tissues [102]. All methods allow successful coregistering of functional information within the framework of anatomical structures. Although these approaches are mainly applied preclinically, as multimodal imaging integrates the strengths of different modalities to provide comprehensive information or to assess biological processes in their anatomical context it

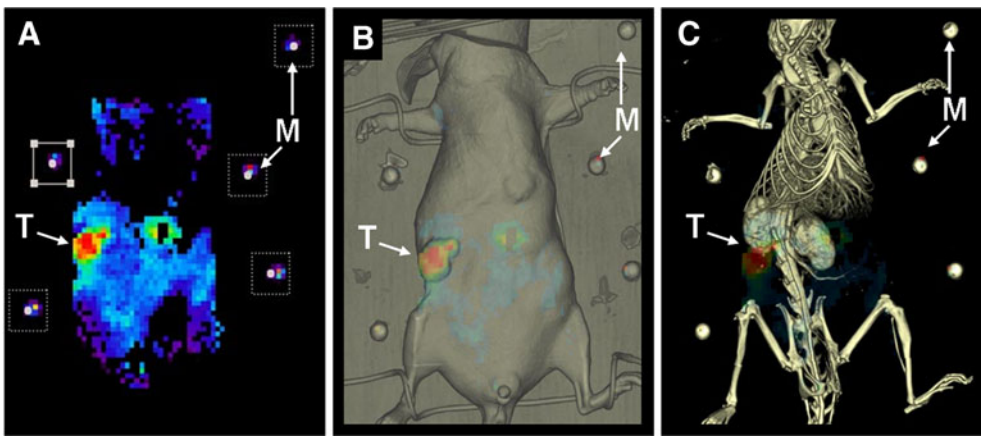

Fig. 7 Landmark-based fusion of 2-D NIRF image and 3-D fpVCT data set. **a** NIRF image acquired with the Optix MX2 24 h after application of a Cy5.5 labelled tumour-specific antibody into a mouse with a subcutaneous tumour (*T*). Strong fluorescence is detected over the tumour. Note the fiducial markers (*M*) that are filled with both NIRF dye and iodinated contrast agent. **b** Image fusion of the same NIRF image and the surface representation of the fpVCT scan acquired 28 s after intravenous injection of 150 µl Isovist 300 (Bayer Schering Pharma, Berlin, Germany), shows the exact shape and location of the tumour. **c** Image fusion as shown in (**b**); the fpVCT scan is depicted as volume-rendering of the skeleton and blood vessels filled with iodinated contrast agent

has also a great potential to be a valuable tool in diagnosis and treatment of paediatric disease.

Clinical applications of OI

OI techniques represent easy, inexpensive and harmless tools to study, diagnose or monitor disease development and progression. Whereas the role of BLI is restricted to preclinical examination in animal models, the routine use of fluorescence-based technologies in the clinic is expanding. So far, mainly microscopic and micro(endo)scopic techniques are used for diagnostic purposes and during surgical procedures.

Confocal endomicroscopes have already been applied in patients, for example to elucidate malignant lesions or inflammatory processes of the human skin, cervix and oral cavity, or to endomicroscopically explore the gastric and colonic mucosae, biliary tract and the proximal and distal respiratory system [103]. High-resolution imaging by multiphon tomography is performed in humans for a variety of skin diseases [104].

Due to the significant improvement in OCT imaging performance in recent years e.g., the development of ultrabroad-bandwidth and tunable light sources, hand-held systems as well as the enhancement of image contrast and noninvasive depth-resolved functional imaging, OCT has been found more and more its way into clinical application in paediatric patients [105]. For example, in paediatric ophthalmology, OCT has already been used to image the retina in order to diagnose infants with genetic disorders, e.g., congenital X-linked retinoschisis [106, 107] and autosomal-recessive neurocutaneous Sjögren-Larsson syndrome, by studying morphological changes in the macula of children with a crystalline macular dystrophy [108]. In neurofibromatosis-2, neurologically asymptomatic children with a severe phenotype can also be early diagnosed by detection of epiretinal membranes using OCT [109]. OCT may also contribute to monitoring juvenile glaucoma progression [110]. The development of easy-to-handle hand-held devices, such as a spectral domain OCT, provides a further possibility to assess pathological changes of the infant eye [111]. In dermatology, OCT combined with multiphoton microscopy enables beside the generation of wide-field images of skin lesions with depth information up to 2 mm, the generation of high-resolution stacks of horizontal multiphoton images of the region of interest. This allows not only early detection of skin cancer, but also investigation of inflammatory and autoimmune diseases as well as detection of vascular lesions and deformation in children [104]. Furthermore, OCT has been shown to be a helpful diagnostic tool in children with mild or marked villous atrophy for diagnosing coeliac disease during upper gastrointestinal endoscopy, avoiding biopsies [112, 113].

Another interesting technique, NIR spectroscopy (NIRS) that measures the wavelength and intensity of the absorption of NIR light by intact tissue, is increasingly used as a noninvasive, inexpensive and portable method to measure blood flow or tissue oxygenation and thereby to study, for example, functional brain activity in infants. Since haemoglobin, myoglobin, and cytochrome c oxidase are the only biological compounds to exhibit variable absorption of NIR light in response to changes in oxygen availability, NIRS can determine changes in tissue oxygen and haemodynamics [114]. For example, frequency-domain NIRS was shown in a pilot study to be useful to identify neonates with brain injury by assessing increased cerebral blood volume and oxygen consumption [115]. Furthermore, combined with diffusion correlation spectroscopy that provides a measure of tissue perfusion based on the movement of scatter, frequency-domain NIRS has been shown to be a safe and quantitative bedside method to monitor cerebral tissue oxygenation, cerebral blood volume and cerebral blood flow index in human premature neonates in the first 6 weeks of life [116]. Since fluorescence and diffuse reflectance spectroscopy provide noninvasive methods to assess haemodynamics and metabolism of the brain they can be used for delineation of the true resection margin of an epileptic cortical lesion in epilepsy surgery [117].

In several disciplines of surgical oncology, intraoperative OI facilitates detection of residual tumour tissue at the resection edge. For example, time-domain OCT allows distinction between normal brain, diffusely invaded brain tissue and solid tumour and thereby the discrimination of the tumour-to-brain interface [118]. Intraoperative brain OI of 5-aminolevulinic acid, an optical dye that is metabolized preferentially by tumour cells, has been shown to allow precise resections of malignant gliomas [119, 120] and a benign paediatric brain tumour [121]. Also ICG fluorescence angiography offers potential for a reliable intraoperative assessment of paediatric cardiac surgery, especially when complicated blood vessel reconstructions and delicate anastomoses are needed [122]. The method appears safe in children and allows the intraoperative assessment of vessels and anastomotic patency. The results are comparable to common procedures such as echocardiograms and cardiac cineangiograms [122].

In the future, image-guided intraoperative NIRF imaging in combination with specific molecular probes targeting biomarkers of paediatric tumours will assist the paediatric surgeon and even the pathologist during oncological surgery. Multiple targeted molecular probes have been already evaluated for their suitability to intraoperatively assess a variety of tumour

entities including lymph node mapping [123]. In paediatric malignancies, the most common biomarkers in clinical use are alpha-fetoprotein in liver and yolk sac tumours, chorionic gonadotropin in germ cell tumours and catecholamines and neuron-specific enolase in neuroblastoma. Hopefully, with more studies aimed at the discovery of potential protein biomarkers for paediatric tumours, novel probes targeting tumour-associated proteins will emerge in the near future.

Conclusion

In vivo OI with fluorescence or bioluminescence as sources of contrast have become powerful tools to unravel mechanisms underlying diseases (including paediatric disorders), to diagnose and design and to evaluate the efficacy of novel therapeutic concepts. The increasing availability of improved bioluminescent reporter systems, NIRF dyes and targeted or activatable fluorescent probes, as well as the development of multifunctional probes in combination with multimodal imaging devices and mouse models of paediatric tumours or genetic disorders will have a significant impact in providing insights in molecular events of paediatric diseases. Since fluorescence-based imaging techniques have limited depth penetration and limited quantification, FRI and FMT are still mainly used experimentally, although they have growing roles in clinical translation especially in analyzing structures close to an accessible tissue surface. Most promising are endoscopic fluorescence-based technologies that are less hampered by the low penetration depth offering effective and minimally-invasive procedures for future application in patients. The development of appropriate low-cost instrumentation and the design and clinical approval of novel targeted probes will further facilitate the translation into the clinic.

References

1. Hilderbrand SA, Weissleder R (2010) Near-infrared fluorescence: application to in vivo molecular imaging. Curr Opin Chem Biol 14:71–79
2. Ntziachristos V, Ripoll J, Wang LV et al (2005) Looking and listening to light: the evolution of whole-body photonic imaging. Nat Biotechnol 23:313–320
3. Zacharakis G, Shih H, Ripoll J et al (2006) Normalized transillumination of fluorescent proteins in small animals. Mol Imaging 5:153–159
4. Napp J, Dullin C, Muller F et al (2010) Time-domain in vivo near infrared fluorescence imaging for evaluation of matriptase as a potential target for the development of novel, inhibitor-based tumor therapies. Int J Cancer 127:1958–1974
5. McCormack E, Micklem DR, Pindard LE et al (2007) In vivo optical imaging of acute myeloid leukemia by green fluorescent protein: time-domain autofluorescence decoupling, fluorophore quantification, and localization. Mol Imaging 6:193–204
6. Montet X, Nzich V, Grimm J et al (2005) Tomographic fluorescence mapping of tumor targets. Cancer Res 65:6330–6336
7. Ntziachristos V, Schellenberger EA, Ripoll J et al (2004) Visualization of antitumor treatment by means of fluorescence molecular tomography with an annexin V-Cy5.5 conjugate. Proc Natl Acad Sci USA 101:12294–12299
8. Montet X, Figueiredo JL, Alencar H et al (2007) Tomographic fluorescence imaging of tumor vascular volume in mice. Radiology 242:751–758
9. Haller J, Hyde D, Deliolanis N et al (2008) Visualization of pulmonary inflammation using noninvasive fluorescence molecular imaging. J Appl Physiol 104:795–802
10. Tan Y, Jiang H (2008) Diffuse optical tomography guided quantitative fluorescence molecular tomography. Appl Opt 47:2011–2016
11. Gerger A, Hofmann-Wellenhof R, Sanronigg H et al (2009) In vivo confocal laser scanning microscopy in the diagnosis of melanocytic skin tumours. Br J Dermatol 160:475–481
12. Wang BG, Konig K, Halbhuber KJ (2010) Two-photon microscopy of deep intravital tissues and its merits in clinical research. J Microsc 238:1–20
13. Drexler W, Fujimoto JG (2008) State-of-the-art retinal optical coherence tomography. Prog Retin Eye Res 27:45–88
14. Huang D, Swanson EA, Lun CP et al (1991) Optical coherence tomography. Science 254:1178–1181
15. Wang X, Pang Y, Ku G et al (2003) Noninvasive laser-induced photoacoustic tomography for structural and functional in vivo imaging of the brain. Nat Biotechnol 21:803–806
16. Zhang HF, Maslov K, Stoica G et al (2006) Functional photoacoustic microscopy for high-resolution and noninvasive in vivo imaging. Nat Biotechnol 24:848–851
17. Morise H, Shimomura O, Johnson FH et al (1974) Intermolecular energy transfer in the bioluminescent system of Aequorea. Biochemistry 13:2656–2662
18. Prasher DC, Eckenrode VK, Ward WW et al (1992) Primary structure of the Aequorea victoria green-fluorescent protein. Gene 111:229–233
19. Hoffman RM (2009) Imaging cancer dynamics in vivo at the tumor and cellular level with fluorescent proteins. Clin Exp Metastasis 26:345–355
20. Shaner NC, Steinbach PA, Tsien RY (2005) A guide to choosing fluorescent proteins. Nat Methods 2:905–909
21. Pauli J, Brehm R, Spieles M et al (2010) Novel fluorophores as building blocks for optical probes for in vivo near infrared fluorescence (NIRF) imaging. J Fluoresc 20:681–693
22. Resch-Genger U, Grabolle M, Cavaliere-Jarocot S et al (2008) Quantum dots versus organic dyes as fluorescent labels. Nat Methods 5:763–775
23. Weissleder R, Pittet MJ (2008) Imaging in the era of molecular oncology. Nature 452:580–589
24. Shu X, Royant A, Lin MZ et al (2009) Mammalian expression of infrared fluorescent proteins engineered from a bacterial phytochrome. Science 324:804–807
25. Shcherbo D, Merzlyak EM, Chepurnykh TV et al (2007) Bright far-red fluorescent protein for whole-body imaging. Nat Methods 4:741–746
26. Zhou L, El-Deiry WS (2009) Multispectral fluorescence imaging. J Nucl Med 50:1563–1566
27. Tung CH (2004) Fluorescent peptide probes for in vivo diagnostic imaging. Biopolymers 76:391–403

28. Kubota K, Kita J, Shimoda M et al (2006) Intraoperative assessment of reconstructed vessels in living-donor liver transplantation, using a novel fluorescence imaging technique. J Hepatobiliary Pancreat Surg 13:100–104
29. Dzurinko VL, Gurwood AS, Price JR (2004) Intravenous and indocyanine green angiography. Optometry 75:743–755
30. Altinoglu EI, Russin TJ, Kaiser JM et al (2008) Near-infrared emitting fluorophore-doped calcium phosphate nanoparticles for in vivo imaging of human breast cancer. ACS Nano 2:2075–2084
31. Park K, Lee S, Kang E et al (2009) New Generation of Multifunctional Nanoparticles for Cancer Imaging and Therapy. Adv Funct Mater 19:1553–1566
32. Pirollo KF, Chang EH (2008) Does a targeting ligand influence nanoparticle tumor localization or uptake? Trends Biotechnol 26:552–558
33. Hamidi M, Azadi A, Rafiei P (2006) Pharmacokinetic consequences of pegylation. Drug Deliv 13:399–409
34. Choi HS, Liu W, Liu F et al (2010) Design considerations for tumour-targeted nanoparticles. Nat Nanotechnol 5:42–47
35. Herbort CP, LeHoang P, Guex-Crosier Y (1998) Schematic interpretation of indocyanine green angiography in posterior uveitis using a standard angiographic protocol. Ophthalmology 105:432–440
36. Brancato R, Trabucchi G (1998) Fluorescein and indocyanine green angiography in vascular chorioretinal diseases. Semin Ophthalmol 13:189–198
37. Raabe A, Beck J, Gerlach R et al (2003) Near-infrared indocyanine green video angiography: a new method for intraoperative assessment of vascular flow. Neurosurgery 52:132–139
38. Lewis JD, Destito G, Zijlstra A et al (2006) Viral nanoparticles as tools for intravital vascular imaging. Nat Med 12:354–360
39. Lee PJ, Peyman GA (2003) Visualization of the retinal and choroidal microvasculature by fluorescent liposomes. Methods Enzymol 373:214–233
40. Larson DR, Zipfel WR, Williams RM et al (2003) Water-soluble quantum dots for multiphoton fluorescence imaging in vivo. Science 300:1434–1436
41. Scheuer W, Friess T, Burtscher H et al (2009) Strongly enhanced antitumor activity of trastuzumab and pertuzumab combination treatment on HER2-positive human xenograft tumor models. Cancer Res 69:9330–9336
42. Hilger I, Leistner Y, Berndt A et al (2004) Near-infrared fluorescence imaging of HER-2 protein over-expression in tumour cells. Eur Radiol 14:1124–1129
43. Ogawa M, Kosaka N, Choyke PL et al (2009) In vivo molecular imaging of cancer with a quenching near-infrared fluorescent probe using conjugates of monoclonal antibodies and indocyanine green. Cancer Res 69:1268–1272
44. Dullin C, Zientkowska M, Napp J et al (2009) Semiautomatic landmark-based two-dimensional-three-dimensional image fusion in living mice: correlation of near-infrared fluorescence imaging of Cy5.5-labeled antibodies with flat-panel volume computed tomography. Mol Imaging 8:2–14
45. Stuhmer W, Alves F, Hartung F et al (2006) Potassium channels as tumour markers. FEBS Lett 580:2850–2852
46. Holliger P, Hudson PJ (2005) Engineered antibody fragments and the rise of single domains. Nat Biotechnol 23:1126–1136
47. Matsumura Y, Maeda H (1986) A new concept for macromolecular therapeutics in cancer-chemotherapy - mechanism of tumoritropic accumulation of proteins and the antitumor agent smancs. Cancer Res 46:6387–6392
48. van Osdol W, Fujimori K, Weinstein JN (1991) An analysis of monoclonal antibody distribution in microscopic tumor nodules: Consequences of a "binding site barrier." Cancer Res 51:4776
49. Rudnick SI, Adams GP (2009) Affinity and avidity in antibody-based tumor targeting. Cancer Biother Radiopharm 24:155–161
50. Baxter LT, Jain RK (1989) Transport of fluid and macromolecules in tumors. I. Role of interstitial pressure and convection. Microvasc Res 37:77–104
51. Lee SB, Hassan M, Fisher R et al (2008) Affibody molecules for in vivo characterization of HER2-positive tumors by near-infrared imaging. Clin Cancer Res 14:3840–3849
52. Biswal NC, Gamelin JK, Yuan B et al (2010) Fluorescence imaging of vascular endothelial growth factor in tumors for mice embedded in a turbid medium. J Biomed Opt 15:016012
53. Chen WT, Mahmood U, Weissleder R et al (2005) Arthritis imaging using a near-infrared fluorescence folate-targeted probe. Arthritis Res Ther 7:R310–R317
54. Chen XY, Conti PS, Moats RA (2004) In vivo near-infrared fluorescence imaging of integrin a, alpha(v)beta(3) in brain tumor xenografts. Cancer Res 64:8009–8014
55. Veiseh M, Gabikan P, Bahrami SB et al (2007) Tumor paint: A Chlorotoxin: Cy5.5 bioconjugate for intraoperative visualization of cancer foci. Cancer Res 67:6882–6888
56. Weissleder R, Tung CH, Mahmood U et al (1999) In vivo imaging of tumors with protease-activated near-infrared fluorescent probes. Nat Biotechnol 17:375–378
57. Tung CH, Mahmood U, Bredow S et al (2000) In vivo imaging of proteolytic enzyme activity using a novel molecular reporter. Cancer Res 60:4953–4958
58. Jaffer FA, Kim DE, Quinti L et al (2007) Optical visualization of cathepsin K activity in atherosclerosis with a novel, protease-activatable fluorescence sensor. Circulation 115:2292–2298
59. Messerli SM, Prabhakar S, Tang Y et al (2004) A novel method for imaging apoptosis using a caspase-1 near-infrared fluorescent probe. Neoplasia 6:95–105
60. Bremer C, Tung CH, Weissleder R (2001) In vivo molecular target assessment of matrix metalloproteinase inhibition. Nat Med 7:743–748
61. Law B, Curino A, Bugge TH et al (2004) Design, synthesis, and characterization of urokinase plasminogen-activator-sensitive near-infrared reporter. Chem Biol 11:99–106
62. Kim K, Lee M, Park H et al (2006) Cell-permeable and biocompatible polymeric nanoparticles for apoptosis imaging. J Am Chem Soc 128:3490–3491
63. Lee S, Cha E-J, Park K et al (2008) A near-infrared-fluorescence-quenched gold-nanoparticle imaging probe for in vivo drug screening and protease activity determination. Angew Chem Int Ed Engl 47:2804–2807
64. Yang Z, Zheng S, Harrison WJ et al (2007) Long-circulating near-infrared fluorescence core-cross-linked polymeric micelles: synthesis, characterization, and dual nuclear/optical imaging. Biomacromolecules 8:3422–3428
65. Razkin J, Josserand V, Boturyn D, Jin Z, Dumy P, Favrot M, Coll JL, Texier I (2006) Activatable fluorescent probes for tumour-targeting imaging in live mice. Chem Med Chem 1:1069–1072
66. Tung CH, Zeng Q, Shah K et al (2004) In vivo imaging of beta-galactosidase activity using far red fluorescent switch. Cancer Res 64:1579–1583
67. Gong H, Zhang B, Little G et al (2009) beta-Galactosidase activity assay using far-red-shifted fluorescent substrate DDAOG. Anal Biochem 386:59–64
68. Zhang GJ, Chen TB, Connolly B et al (2009) In vivo optical imaging of LacZ expression using lacZ transgenic mice. Assay Drug Dev Technol 7:391–399
69. Ho NH, Weissleder R, Tung CH (2007) A self-immolative reporter for beta-galactosidase sensing. Chembiochem 8:560–566

70. Gatenby RA, Gillies RJ (2004) Why do cancers have high aerobic glycolysis? Nat Rev Cancer 4:891–899
71. Galande AK, Weissleder R, Tung CH (2006) Fluorescence probe with a pH-sensitive trigger. Bioconjug Chem 17:255–257
72. Povrozin YA, Markova LI, Jatarets AL et al (2009) Near-infrared, dual-ratiometric fluorescent label for measurement of pH. Anal Biochem 390:136–140
73. Zhang Z, Achilefu S (2005) Design, synthesis and evaluation of near-infrared fluorescent pH indicators in a physiologically relevant range. Chem Commun (Camb) 47:5887–5889
74. Stock C, Mueller M, Kraehlung H et al (2007) pH nanoenvironment at the surface of single melanoma cells. Cell Physiol Biochem 20:679–686
75. Urano Y, Asanuma D, Hama Y et al (2009) Selective molecular imaging of viable cancer cells with pH-activatable fluorescence probes. Nat Med 15:104–109
76. Li C, Xia J, Wei X et al (2010) pH-activated near-infrared fluorescence nanoprobe imaging tumors by sensing the acidic microenvironment. Adv Funct Mater 20:2222–2230
77. Gould SJ, Subramani S (1988) Firefly luciferase as a tool in molecular and cell biology. Anal Biochem 175:5–13
78. Wood KV, Lam YA, Seliger HH et al (1989) Complementary DNA coding click beetle luciferases can elicit bioluminescence of different colors. Science 244:700–702
79. Lorenz WW, McCann RO, Longiaru M et al (1991) Isolation and expression of a cDNA-encoding Renilla-reniformis luciferase. Proc Natl Acad Sci USA 88:4438–4442
80. Tannous BA, Kim DE, Fernandez JL et al (2005) Codon-optimized Gaussia luciferase cDNA for mammalian gene expression in culture and in vivo. Mol Ther 11:435–443
81. Sjollema J, Sharma PK, Dijkstra RJ et al (2010) The potential for bio-optical imaging of biomaterial-associated infection in vivo. Biomaterials 31:1984–1995
82. Luker KE, Luker GD (2008) Applications of bioluminescence imaging to antiviral research and therapy: multiple luciferase enzymes and quantitation. Antivir Res 78:179–187
83. Troy T, Jekil-McMullen D, Sambuletti L et al (2004) Quantitative comparison of the sensitivity of detection of fluorescent and bioluminescent reporters in animal models. Mol Imaging 3:9–23
84. Morioka I, Wong RJ, Abate A et al (2006) Systemic effects of orally-administered zinc and tin (IV) metalloporphyrins on heme oxygenase expression in mice. Pediatr Res 59:667–672
85. Zhao H, Wong RJ, Nguyen X et al (2006) Expression and regulation of heme oxygenase isozymes in the developing mouse cortex. Pediatr Res 60:518–523
86. Vooijs M, Jonkers J, Lyons S et al (2002) Noninvasive imaging of spontaneous retinoblastoma pathway-dependent tumors in mice. Cancer Res 62:1862–1867
87. Stubbs MC, Kim YM, Krivtsov AV et al (2008) MLL-AF9 and FLT3 cooperation in acute myelogenous leukemia: development of a model for rapid therapeutic assessment. Leukemia 22:66–77
88. Safran M, Kim WY, O'Connell F et al (2006) Mouse model for noninvasive imaging of HIF prolyl hydroxylase activity: assessment of an oral agent that stimulates erythropoietin production. Proc Natl Acad Sci USA 103:105–110
89. Xie YC, Yin Y, Wiegraebe W et al (2009) Detection of functional haematopoietic stem cell niche using real-time imaging. Nature 457:97–101
90. Carlon M, Toelen J, Van der Perren A et al (2010) Efficient gene transfer into the mouse lung by fetal intratracheal injection of rAAV2/6.2. Mol Ther Jul 27 [Epub ahead of print]
91. Sacco A, Doyonnas R, Kraft P et al (2008) Self-renewal and expansion of single transplanted muscle stem cells. Nature 456:502–506
92. Edinger M, Cao YA, Verneris MR et al (2003) Revealing lymphoma growth and the efficacy of immune cell therapies using in vivo bioluminescence imaging. Blood 101:640–648
93. Cheng JC, Kinjo K, Judelson DR et al (2008) CREB is a critical regulator of normal hematopoiesis and leukemogenesis. Blood 111:1182–1192
94. Kondo A, Goldman S, Vanin EF et al (2009) An experimental brainstem tumor model using in vivo bioluminescence imaging in rat. Childs Nerv Syst 25:527–533
95. Miretti S, Roato I, Taulli R et al (2008) A mouse model of pulmonary metastasis from spontaneous osteosarcoma monitored in vivo by luciferase imaging. PLoS ONE 3:e1828
96. Rousseau J, Escriou V, Perrot P et al (2010) Advantages of bioluminescence imaging to follow siRNA or chemotherapeutic treatments in osteosarcoma preclinical models. Cancer Gene Ther 17:387–397
97. Bridot JL, Faure AC, Laurent S et al (2007) Hybrid gadolinium oxide nanoparticles: multimodal contrast agents for in vivo imaging. J Am Chem Soc 129:5076–5084
98. Jin T, Toshioka Y, Fujii F et al (2008) Gd3+-functionalized near-infrared quantum dots for in vivo dual modal (fluorescence/magnetic resonance) imaging. Chem Commun (Camb) 44:5764–5766
99. Nahrendorf M, Keliher E, Marinelli B et al (2010) Hybrid PET-optical imaging using targeted probes. Proc Natl Acad Sci USA 107:7910–7915
100. Nahrendorf M, Waterman P, Thurber G et al (2009) Hybrid in vivo FMT-CT imaging of protease activity in atherosclerosis with customized nanosensors. Arterioscler Thromb Vasc Biol 29:1444–1451
101. Ntziachristos V (2009) Optical imaging of molecular signatures in pulmonary inflammation. Proc Am Thorac Soc 6:416–418
102. Jiao S, Xie Z, Zhang HF et al (2009) Simultaneous multimodal imaging with integrated photoacoustic microscopy and optical coherence tomography. Opt Lett 34:2961–2963
103. Thiberville L, Salaun M, Lochkar S et al (2009) Human in vivo fluorescence microimaging of the alveolar ducts and sacs during bronchoscopy. Eur Respir J 33:974–985
104. Konig K, Speicher M, Buckle R et al (2009) Clinical optical coherence tomography combined with multiphoton tomography of patients with skin diseases. J Biophotonics 2:389–397
105. Kiernan DF, Mieler WF, Hariprasad SM (2010) Spectral-domain optical coherence tomography: a comparison of modern high-resolution retinal imaging systems. Am J Ophthalmol 149:18–31
106. Gerth C, Zawadzki RJ, Heon E et al (2009) High-resolution retinal imaging in young children using a handheld scanner and Fourier-domain optical coherence tomography. J AAPOS 13:72–74
107. Dhingra S, Patel CK (2010) Diagnosis and pathogenesis of congenital X-linked retinoschisis with optical coherence tomography. J Pediatr Ophthalmol Strabismus 47:105–107
108. Fuijkschot J, Cruysberg JR, Willemsen MA et al (2008) Subclinical changes in the juvenile crystalline macular dystrophy in Sjogren-Larsson syndrome detected by optical coherence tomography. Ophthalmology 115:870–875
109. Sisk RA, Berrocal AM, Schefler AC et al (2010) Epiretinal membranes indicate a severe phenotype of neurofibromatosis type 2. Retina 30:S51–58
110. Mrugacz M, Bakunowicz-Lazarczyk A (2005) Optical coherence tomography measurement of the retinal nerve fiber layer in normal and juvenile glaucomatous eyes. Ophthalmologica 219:80–85
111. Scott AW, Farsiu S, Enyedi LB et al (2009) Imaging the infant retina with a hand-held spectral-domain optical coherence tomography device. Am J Ophthalmol 147(364–373):e2
112. Masci E, Mangiavillano B, Barera G et al (2009) Optical coherence tomography in pediatric patients: a feasible technique for diagnosing celiac disease in children with villous atrophy. Dig Liver Dis 41:639–643

113. Cucchiara S, Di Nardo G (2009) Optical coherence tomography in children with coeliac disease. Dig Liver Dis 41:630–631
114. Lloyd-Fox S, Blasi A, Elwell CE (2010) Illuminating the developing brain: the past, present and future of functional near infrared spectroscopy. Neurosci Biobehav Rev 34:269–284
115. Grant PE, Roche-Labarbe N, Surova N et al (2009) Increased cerebral blood volume and oxygen consumption in neonatal brain injury. J Cereb Blood Flow Metab 29:1704–1713
116. Roche-Labarbe N, Carp SA, Surova N et al (2010) Noninvasive optical measures of CBV, StO2, CBF index, and rCMRO2 in human premature neonates' brains in the first six weeks of life. Hum Brain Mapp 31:341–352
117. Bhatia S, Ragheb J, Johnson M et al (2008) The role of optical spectroscopy in epilepsy surgery in children. Neurosurg Focus 25:E24
118. Bohringer HJ, Lankenau E, Stellmacher F et al (2009) Imaging of human brain tumor tissue by near-infrared laser coherence tomography. Acta Neurochir (Wien) 151:507–517, discussion 517
119. Nabavi A, Thurm H, Zountas B et al (2009) Five-aminolevulinic acid for fluorescence-guided resection of recurrent malignant gliomas: a phase ii study. Neurosurgery 65:1070–1076, discussion 1076–1077
120. Widhalm G, Wolfsberger S, Minchev G et al (2010) 5-Aminolevulinic acid is a promising marker for detection of anaplastic foci in diffusely infiltrating gliomas with nonsignificant contrast enhancement. Cancer 116:1545–1552
121. Ruge JR, Liu J (2009) Use of 5-aminolevulinic acid for visualization and resection of a benign pediatric brain tumor. J Neurosurg Pediatr 4:484–486
122. Kogon B, Fernandez J, Kanter K et al (2009) The role of intraoperative indocyanine green fluorescence angiography in pediatric cardiac surgery. Ann Thorac Surg 88:632–636
123. Tanaka E, Choi HS, Fujii H et al (2006) Image-guided oncologic surgery using invisible light: completed pre-clinical development for sentinel lymph node mapping. Ann Surg Oncol 13:1671–1681